BENEFITS AND DRAWBACKS OF LASER REMOTE SENSING IN ATMOSPHERIC RESEARCH

Doina NICOLAE[1], Camelia TALIANU[2], Anca NEMUC[3], Emil CÂRSTEA[4]

Sistemele lidar sunt utilizate deseori în studiul atmosferei, ca şi în topografie, oceanografie, silvicultură şi aeronautică. Sistemele lidar sunt instrumente optoelectronice complexe, având în consecinţă atât limitări teoretice cât şi tehnologice. Informaţiile extrase din date lidar trebuie de aceea analizate în strânsă corelaţie cu posibilităţile tehnice ale instrumentului, ca şi cu cele de procesare a datelor. Această lucrare prezintă avantajele şi dezavantajele utilizării teledetecţiei laser în studiul atmosferei, punând accent pe nivelul de încredere care poate fi acordat datelor lidar şi parametrilor extraşi din prelucrarea acestora. Soluţii practice noi pentru optimizarea instrumentului şi a lanţului de procesare sunt de asemenea prezentate..

Lidars are often used in atmospheric research, as well as in topography, oceanography, forestry and air transportation. Lidars are complex optoelectronique systems, having by consequence technological but also theoretical limitations. The information extracted from lidar data should be therefore closely analyzed in relation with instrumental and processing capabilities. This paper presents advantages and drawbacks of using laser remote sensing in atmospheric science, emphasizing the level of trust that can be given to lidar data and derived parameters. Moreover, some new practical solutions for the optimization of the instrument and data processing chain are also presented.

Keywords: lidar, atmosphere, laser, aerosol

1. Introduction

The atmosphere consists of components that are in relatively fixed abundance in the lower atmosphere such as oxygen and nitrogen which together make up ~97% of the mass of the atmosphere and the trace gasses such as argon, neon, helium that taken all together account for approximately 1% of atmospheric mass. In most of the lower atmosphere, CO2 is also well-mixed (with a value currently of ~370 ppm and increasing by ~1ppm/yr) except in the boundary layer where its concentration can change by many 10's of ppm during the diurnal photosynthetic cycle. Gaseous water (water vapor) is not well-mixed in the

[1] Physicist, National Institute for Optoelectronics, Romania
[2] Mathematician., National Institute for Optoelectronics, Romania
[3] Physicist, National Institute for Optoelectronics, Romania
[4] Eng. Physicist, National Institute for Optoelectronics, Romania

atmosphere and can change its concentration by an order of magnitude in small time and space scales. On average water vapor comprises from 0-2% of the mass of the atmosphere. Various atmospheric particles are also not well-mixed and have lifetimes in suspension in the atmosphere from a day to ~2 weeks typically.

Human activity during industrial era has perturbed the Earth's energy balance by altering the properties of the atmosphere and by modifying the biosphere. Perturbations of the energy balance of the Earth, considered as a thermodynamic system, would be expected to lead to significant changes of the climate. In recent years, an increasing number of possible human-related climate change mechanisms have begun to be investigated and quantified.

Characterization of the real atmosphere requires a large number of meteorological parameters such as temperature, humidity, wind directions, and in addition, variations in chemical composition and the presence of pollutants, which can undergo rapid local changes, in particular over urban areas.

Conform to the diffraction theory, an obstacle could be "seen" by an electromagnetic wave having a wavelength on the same magnitude as the geometric dimension of the obstacle. So, using a light beam (wavelength nm, μm) one can detect atmospheric components, which are "invisible" for other sounding waves. Based on this theory, optical remote sensing techniques were developed in the last 20 years. Due to the high speed of light and rapid acquisition, these instruments provide vertical profiles of atmospheric parameters in real time. A lot of phenomena are produced at the interaction between a light beam and atmospheric constituents, most of these phenomena being specific to the constituent's type, and can be used to derive many parameters. Very important among optical remote sensing techniques are **LIDARs** (**LI**ght **D**etection **A**nd **R**anging), are instruments which use pulsed or continuous lasers to sound high altitudes in the atmosphere, as they are characterized by high sensitivity and a long range of penetration.

The name "LIDAR" pre-dated the invention of the laser because of other light based techniques using arc-lamp searchlights for atmospheric profiling that started much earlier with Synge (1930) **Error! Reference source not found.**, Hulbert (1937) 0, Johnson (1939) 0 and Elterman (1954) 0 using a carbon arc lamp searchlight, followed by Friedland (1956) 0 using a pulsed search light. It's also interesting to note early passive techniques that were developed to profile atmospheric aerosols by observing the sky during sunset.

After the development of new lasers and photodetectors in the following years, various types of ground-based lidar systems (including ceilometers) have been continuously used to probe the earth's atmosphere and to detect a variety of air pollutants, such as O_3, NOx, SO_2, Hg, toluene, benzene and measure aerosol optical properties (optical depth, spatial distribution and layering, diurnal

variation, etc.), as described by Kölsch (1989) 0, Measures (1992) 0, Bösenberg et al., (2003) 0, Kovalev and Eichinger (2004) 0.

This paper analyzes the level of trust that can be given to lidar data and derived parameters in relation with instrumental and processing capabilities. New practical solutions for the optimization of the instrument and data processing chain are also presented.

2. The instrument

Lidar is an active remote sensing technique based on the emission of laser pulses (ns) into the atmosphere and the analysis of the return signal. Depending on the emitted and selected wavelength at the detection, different characteristics of air pollutants can be measured. The photons scattered by the atmospheric particles are collected by a receiving optical telescope. To ensure a good wavelength selection of the lidar signals, narrow-band interference filters are used one for each detected wavelength. The selected radiation is focused on a photomultiplier (PMT) – for visible and UV light, respectively on an avalanche photodiode (APD) – for IR light, which convert the optical signal into electrical signal. The distance between the lidar system and the atmospheric target can be calculated measuring the delay time between the emitted and the received laser pulses. Thus, range resolved measurements of the desired air pollutants or atmospheric parameters can be obtained.

a) b)

Fig. 1. Various designs of lidar systems : a) 2-wavelengths elastic backscatter lidar (LiSA at INOE) ; b) multiwavelengths Raman lidar (RALI at INOE)

Depending on the system design, lidars can measure the backscatter coefficient profiles of aerosols (elastic backscatter lidar), extinction coefficient profile of aerosols (Raman lidar), particle depolarization (depolarization lidar), concentration of various gaseous compounds (differential absorption lidar), organic compounds (fluorescence lidar), speed and wind direction (Doppler lidar). The design of the system is so different for these applications, that no actual instrument can perform all the tasks together.

LiSA (Fig. 1 a) is a 2-wavelenghts elastic backscatter lidar (emitted wavelengths: 1064 and 532nm), generally used for measurements in the lower troposphere (5-6km maximum range and at 3 m range resolution). The backscattered signals (1064 and 532nm) are collected through an optical telescope, and further acquired and digitized in the analog mode using fast transient recorders. Because Nd:YAG lasers have prove their efficiency from energetic and pointing stability point of view, most of aerosol lidar systems are built starting from the fundamental and the 2nd and/or 3rd harmonics of the Nd:YAG laser.

RALI (Fig. 1 b) is a multiwavelength Raman lidar, used for measurements in the lower and upper troposphere (15-20km maximum range at 3.75m range resolution). The laser radiation is emitted at 1064, 532 and 355nm and collected at 1064, 532p, 532s, 355, 607, 387 and 408nm. The 607 and 387nm radiation corresponds to the Raman lines of Nitrogen, excited with 532 and 355 nm respectively. The 408nm radiation corresponds to the Raman line of water vapor excited with 355nm. Almost all channels have both analog and photon counting detection, in order to increase the range (analog for the lower troposphere and photon counting for the upper troposphere).

3. Methodology

In case of aerosols the number of unknown parameters is quite important, making difficult the retrieval of concentration profile, for example. The detected signal of the lidar system is the result of the molecular and aerosol scattering. So, the parameters that can be first derived are the backscattering coefficient and the extinction coefficient. In case of LiSA, which has only elastic backscatter channels, the only parameter that can be derived with a good accuracy is the backscatter coefficient. This is due to the non-determination of the elastic lidar equation (1 equation and 2 unknown parameters: backscatter and extinction coefficient):

$$RCS(\lambda_L, Z) = C_S(\lambda_L, Z) \cdot \beta_t(\lambda_L, Z) \cdot \exp\left[-2\int_0^Z \alpha_t(\lambda_L, z)dz\right] + b(\lambda_L, Z) \quad (1)$$

where λ_L is the laser emitted – detected wavelength (i.e. λ_L = 355, 532 and 1064 nm), C_S is a system function, β_t is the total backscatter coefficient, α_t is the total

extinction coefficient and *b* is the background signal (electronic, solar-moon induced noise, light contamination sources, homogeneous or shaped offsets of the detector's base line, etc). The β_t [$m^{-1}sr^{-1}$] and α_t [m^{-1}] coefficients may be expressed as the sum of the aerosols (a) and molecular (m) contributions:

$$\begin{aligned}\beta_t(\lambda_L,Z) &= \beta_a(\lambda_L,Z)+\beta_m(\lambda_L,Z)+\beta_{tracegases}(\lambda_L,Z)\\ \alpha_t(\lambda_L,Z) &= \alpha_a(\lambda_L,Z)+\alpha_m(\lambda_L,Z)+\alpha_{abs}(\lambda_L,Z)\end{aligned} \quad (2)$$

All molecular parameters can be calculated with sufficient accuracy from ground values of pressure and temperature using the atmospheric model 0. For the reference value of backscattering coefficient a molecular assumed value at high altitude can be considered, but for solving the equation for the aerosol backscatter, the lidar ratio profile must be evaluated. LR_a depends on the aerosol microphysics and can vary between less than 10 sr (ice crystals) and more than 100 sr (heavily polluted air) 0. It depends on humidity and aerosol mixture and therefore, on altitude. One possibility is to measure LR_a using either high spectral resolution lidar 0, 0, or a multiwavelength Raman lidar 0.

In case of a Raman lidar, the parameter that can be derived directly is the extinction coefficient, based on the Raman lidar equation:

$$RCS^R(Z) = C^R(Z)\cdot\beta^R(Z)\cdot\exp\left\{-\int_{Z_{\min}}^{Z}\left[\alpha_m^L(z)+\alpha_a^L(z)+\alpha_m^R(z)+\alpha_a^R(z)\right]dz\right\} \quad (3)$$

By combining elastic and Raman channels, both backscatter and extinction coefficient (consequently that lidar ratio also) can be therefore derived with a good accuracy, since we have 2 equation and 2 unknown parameters. But even so, LR_a can only be measured for the lowest part of the profile, where the Raman signal is strong enough, and only when the background radiation is small enough to have a significant signal to noise ratio (nighttime generally). For this reason, additional methods to eliminate non determination in Lidar equation were developed 0. Optical parameters that can be derived, beside the backscatter and extinction coefficient, are: *1) Angstrom coefficients* - describe the wavelength dependency of the extinction coefficient); *2) Depolarization ratio* - calculated as the ratio of cross (c) to parallel (p) polarization states of the backscatter radiation relative to the initial linear polarization plan of the emitted laser light. The depolarization ratio may be used to distinguish between spherical (e.g. water droplets, with low depolarization ratios) or nonspherical (e.g. ice crystals, with high depolarization ratios). It can be also indirectly an indicator about the hydration rate (humid or dry) of aerosols or even about their lifetime (aged or fresh) and their physical composition (water or ice content); *3) Aerosols' optical depth or thickness* - the extinction coefficient integrated on an atmosphere path; *4) Aerosols single-scattering albedo* - the scattering to extinction ratio.

More then optical, microphysical parameters of aerosols can be derived by processing lidar data (some additional information is still required) 0: *1) Surface-area weighted effective radius*; *2) Total surface-area concentration, the total volume concentration, and the total number concentration of particles*; *3) The complex refractive index of aerosols*. Unfortunately, even in case of multiwavelength lidars, there are no exact methods to invert the equations in order to derive the microphysical parameters. The most probable mathematical solution can be obtained based on existing databases and sophisticated algorithms 0.

Beyond the difficulties of extracting information from lidar data (which give the theoretical limitations of laser remote sensing), technological limitations must be considered. Any optoelectronic instrument is limited by the noise (background radiation and electronic noise of the components), but in case of lidars the geometry of the system also introduces limitations. There are 2 basic designs of lidars: coaxial and biaxial. In case of coaxial systems, the alignment of laser and telescope axis is not an issue, but the signal is reduced by the obstruction of the secondary mirror of the telescope. This reduces drastically the maximum range of the instrument. In case of biaxial systems, the signal is much stronger, but the alignment of laser and telescope axis can introduce problems. First of all, due to the distance between the 2 axes, biaxial lidars have a "blind" region in the lower part of the profile. This region is generally between 300 and 1000m, depending on the geometry of the instrument. Second, a perfect alignment between telescope axis and laser beam can never be achieved, so the maximum range is dependent on the alignment as well as on the laser power or the telescope field of view.

The optimization of the lidar signal has to provide solutions for testing and improving the alignments, reducing and filtering the electronic noise, but also for background and range correction, overlap correction and calibration.

4. Results

4.1. Method for testing the alignments

One of the methods developed for the alignment testing is the telescope cover test. In a perfect lidar system the backscattered rays from all lidar ranges within the measurement range have the same transmission in the optical system. In the near range the total transmission decreases, because some rays are vignietted by the field-of-view aperture and/or other apertures, which results in the overlap function. At the same time rays with large incident angles in the telescope - and therefore with large incident angles on interference filters etc. - can have reduced transmission due to the angular wavelength shift with incident angle of the interference filters.

We can use this behavior to check the performance and alignment of the optical system, because the ray-bundles from different parts of the telescope aperture travel through the optical setup in different paths and with different incident angles on the optical elements.

When we compare the range depended lidar signals of rays-bundles from different parts of the telescope aperture we can find the differences in the transmission losses due to vignietting and due to the angular dependent transmission of the different ray paths. We can do this by covering the telescope aperture with opaque cardboard for example and subsequently measuring only ray-bundles from one of the eight or four sections shown in figure 2. Eight sections give more information and the differences are more pronounced, but four sections are faster to measure and are probably sufficient for a fast check. The "Top" section is oriented from the telescope optical axis towards the laser optical axis as shown in figure 2. "Left" and "Right" are with respect to viewing towards the telescope.

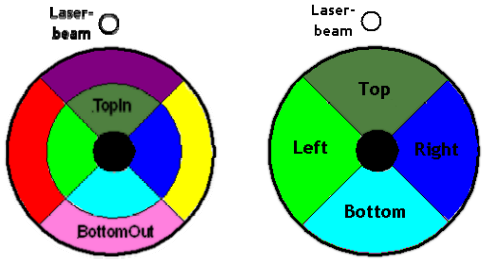

Fig. 2 Telescope cover test: 8 or 4 sectors

Fig. 3 presents some results of the telescope test applied to RALI. It can be seen that first sector that “sees” the laser light is the North sector, the South sector being the last. This shows a good alignment on the N-S axis. In a perfect aligned system, the West and the East sectors should “see” simultaneously the laser beam (the blue and the red line should overlap). At first look on the graphs bellow, it seems that on the W-E axis the system is not well aligned, since the 2 lines don’t overlap. This is not the case, because in several channels (532p and 532s) the curves intersect at some point. A possible explanation is that dust particles are deposited on some parts of the telescope mirror, obstructing the signal.

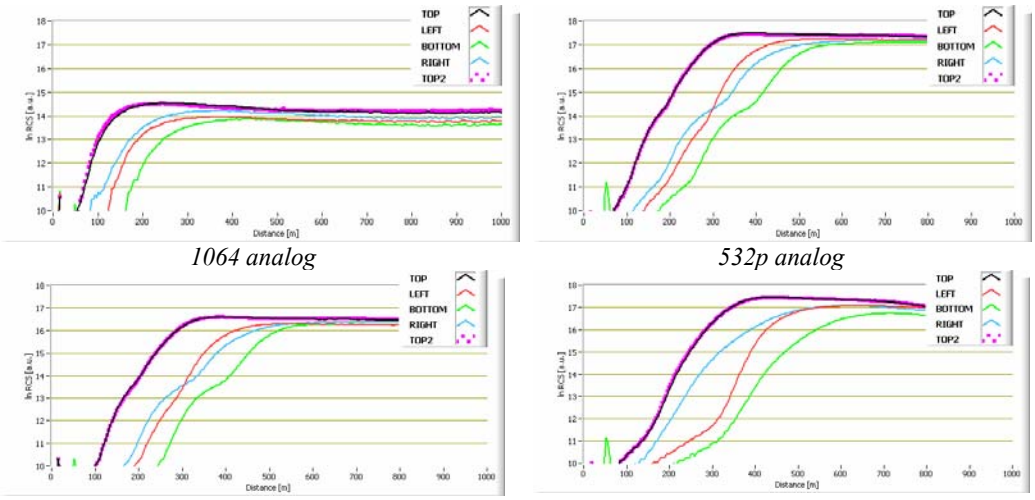

1064 analog *532p analog*

532s analog *355 analog*

Fig. 3 RCS (logarithmic scale) in near range for the 4-sector telescope test applied to elastic channels of RALI

4.1. Method for calculating the overlap function

The algorithm we developed to determine the overlap function works in the hypothesis that the atmospheric transmitance is apriori known (for example from sunphotometer data), or that it can be consideed constant over a relatively long region in the lidar range, including the „blind" region and the region with incomplete overlap.

The overlap function will be calculated up to the limit of Planetary Boundary Layer (PBL). The selected region is divided in 2 intervals: first in the part with incomplete overlap and the second in the part with complete overlap. The point between the 2 intervals is chosen as the point of the first maximum in the lidar signal, Z_s.

Due to the fact the atmospheric transmitance is the same on the entire interval, its contribution to the lidar signal is the same for the incomplete and complete overlap regions. Using the polynomial regression, we can obtain for the overlap function the following equation:

$$O(Z) = \exp\left(\ln RCS(Z) - \sum_{i=0}^{n} A_i Z^i + C \right) \qquad (4)$$

where A_i and n are the coefficients and the degree of the polynom respectively.

The advantage of this algorithm is that no special atmospheric conditions are required and it can be applied on each measurement set, because the polynomial coefficients depend only on the signal. Our tests on real lidar data

proved that the best choice is a 7-deg polynomial fit, but 5 and 6-deg polynoms can also be used.

In figs 4 and 5, 2 examples of retrieved overlap function are shown. Both curves are calculated on LISA signals.

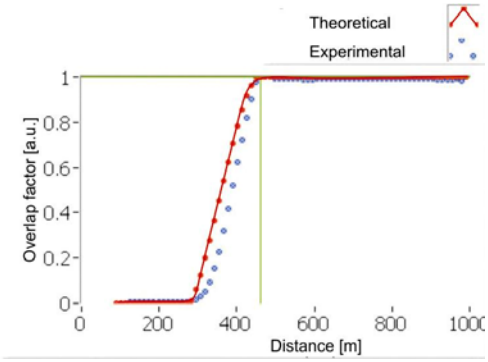

Fig. 4 Theoretical and experimental calculation of the overlap function for a good alignment

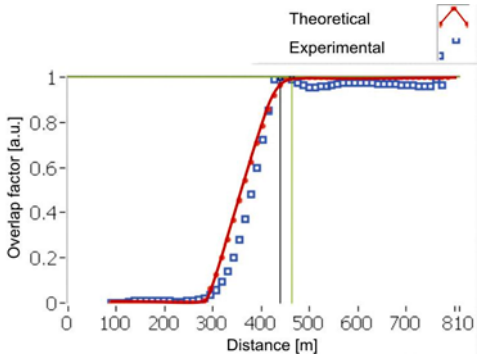

Fig. 5 Theoretical and experimental calculation of the overlap function for a bad alignment ($1*10^{-5}$ deviation from paralelism)

It can be noticed that the experimental retrieval of the overlap function is a much better solution comparing with the theoretical calculations, because no information about the geometry and set-up of the system are necessary. The calculation of the overlap function is important for the pre-processing of the lidar signals for 2 reasons: first of all, using the overlap correction we can derive information about the lower layers in the PBL, which otherwise are „blind"; second, this method can also be used to check the alignment of the system. In case of a misalignment, the anvelope of the overlap function is modiied and the point of full overlap migrates. This can be seen from the form of the overlap function curve, and therefore corrected (see fig.5).

5. Conclusions

Main advantage of lidar is the real time observation of aerosol layering, which can be further used to identify the origin and the path of air mass. This technique has its limitations, but in combination with modeling and complementary techniques more data can be obtained. The accuracy of obtained information is dependent on technical performances of the device and on the sensibility of data processing method, which can be critical in some cases.

In the case of LiSA system (backscattering lidar), increased sensibility and dynamic range was obtained through minimization of relative signal experimental errors (performing system components, high operating stability, alignment testing,

overlap correction) and improvement of pre-processing and processing algorithms.

R E F E R E N C E S

[1] *E.H Synge,* A Method of Investigating the Higher Atmosphere, Phil. Mag. and J. Sci., vol. 9, no. 60, pp. 1014, 1930

[2] *EO Hulbert,* Observations of a Searchlight Beam to an Altitude of 28 Kilometers, J. Opt. Soc. Am. 27, no. 11, pp. 377, 1937

[3] *E.A Johnso., R.C. Meye, R.E. Hopkins, and W.H. Mock,* The Measurement of Light Scattered by the Upper Atmosphere From a Search-Light Beam, J. Opt. Soc. Amer., vol 29, no. 12, pp. 512, 1939

[4] *L. Elterman*, Seasonal Trends of Temperature, Density, and Pressure in the Stratosphere Obtained With the Searchlight-Probing Technique, Geophys. Res. Papers no. 29, Air Force Cambridge Res. Center, 1954

[5] *Friedland S S, Katzenstein J and Zatzick M R , J. Geophys*.Res. 61 415–34, 1956

[6] *H. Kölsch, P. Rairoux, J.P. Wolf and L. Wöste,* Simultaneous NO and NO_2 DIAL measurements using BBO crystals, Appl. Opt., 28, 2052-2056, 1989

[7] *R.M. Measures,* Laser Remote Sensing. Fundamentals and Applications, Krieger Publishing Company, Malabar, Florida, 1992,p. 237

[8] *J. Bösenberg et al*., EARLINET: A European Aerosol Research Lidar Network, MPI Report, 348, Max-Planck-Institut für Meteorologie, Hamburg, Germany, 2003

[9] *V. Kovalev, and V. Eichinger,* Elastic lidar: Theory, Practice and Analysis Methods, Wiley Interscience Publ., New York, USA, 2004

[10] *V.A. Kovalev., H. Mossmuller* , Distortion of particulate extinction profiles measured with lidar in a two-component atmosphere, Appl. Opt. 33, 6499-6507, 1994

[11] *Camelia Talianu, Doina Nicolae, Jeni Ciuciu, Anca Nemuc, E. Carstea, L. Belegante, M. Ciobanu*, New Algorithm For The Retrieval Of Aerosol's Optical Parameters By Lidar Data Inversion, ECMI Series Vol. 11, Springer Verlag, p. 55-62, 2007

[12] *I.* B*alin,* Measurement And Analysis Of Aerosols, Cirrus-Contrails, Water Vapor And Temperature In The Upper Troposphere With The Jungfraujoch Lidar System, Thèse no 2975, Ecole Polytechnique Fédérale de Lausanne, 2004

[13] *J.* A. *Reagan,* et al., Atmospheric particulate properties inferred from lidar and solar radiometer observations compared with simultaneous in situ aircraft measurements: A case study, J. Appl. Met., Vol. 16, 911-928,1977

[14] *P. Piironen and E. W. Eloranta*, Demonstration of a high-spectral-resolution lidar based on an iodine absorption filter, Opt. Lett., Vol.19, 234-236,1994

[15] *, I. Mattis et al*., Dual-wavelength Raman lidar observations of the extinction-to-backscatter ratio of Saharan dust, Geophys.Res. Let., Vol.29, 1306,2002

[16] *C. Bockmann,* Hybrid regularization method for the ill-posed inversion of multiwavelength lidar data in the retrieval of aerosol size distributions. Appl. Opt., 40(9): p. 1329-1342, 2001